Korean J. Chem. Eng., 35(6), 1380-1387 (2018)
DOI: 10.1007/s11814-018-0026-8

pISSN: 0256-1115
eISSN: 1975-7220

Effect of inlet particle arrangement on separating property of a cyclone separator

An-Lin Liu, Yan-Hong Zhang, Liang Ma†, Yi-Mou Wang, and Meng-Ya He

School of Mechanical and Power Engineering, East China University of Science and Technology, Shanghai 200237, China
(*Received 4 May 2017 • accepted 7 February 2018*)

Abstract−Different arrangements of particles on the inlet section exert different effects on the separation property of a cyclone separator. Sorting classifier with different heights was connected in series with a conventional cyclone, positive rotation cyclone, and reverse rotation cyclone respectively, to investigate the effect of particle arrangement on the separation property and inner flow field. Results indicate that the implementation of a sorting classifier increases the pressure drop and energy consumption of a cyclone separator. The taller the sorting classifier, the larger the flow is. The energy consumption in positive rotation cyclone is closer to that in reverse rotation cyclone. Meanwhile, the tangential velocity in inner flow field is higher and the separating property is enhanced. The reverse rotation cyclone relieves the fishhook effect, whereas the positive rotation cyclone eliminates such effect. The reverse and positive rotation cyclones demonstrate an improved separating property for particles smaller and greater than 1 μm, respectively. Moreover, the reverse rotation cyclone demonstrates superior overall separation, but the positive rotation cyclone demonstrates a greater classification effect than the reverse rotation cyclone.

Keywords: Cyclone Separator, Particle Arrangement, Particle Image Velocimetry (PIV), Separating Property

INTRODUCTION

Particles in industrial gases are major atmospheric pollutants and hazardous to human health [1-3]. The advantages of a cyclone separator include structural simplicity, stable property, small floor area, and low energy consumption [4,5]. The cyclone separator, which is widely used in industry, does not jam easily [6-8]. Concentration and granularity of particles in industrial gases greatly affect the separation property of cyclone separator [9,10]. Research currently is focused on improving separation property by ameliorating the structure of a cyclone separator, such as changing the inlet shape [11], inlet angle [12-14], and insertion depth of vortex finder [15]. Sorting classifier arranges the randomly distributed particles with the concentration mainly at 0.5-5.0 mg/L of a gas at the inlet of a cyclone separator [16-18], Fu et al. found that when the height of the sorting classifier was 5a, the sorting performance was the best. However, research on particle sorting and its influence is still in its infancy. Thus far, only few studies have investigated the effect of particle arrangement on the separation property [19-22] and inner flow field of a cyclone separator [23,24]. We investigated three sorting classifiers with different heights. After placement of these series of sorting classifiers in conventional cyclone, positive rotation cyclone, and reverse rotation cyclone, an ordered arrangement of the concentration and granularity of particle was achieved on the inlet section of cyclone. To investigate the effect of particle arrangement on separation property of a cyclone, the pressure drop, separation efficiency, and classification efficiency were calculated and the change of tangential velocity in the flow field was analyzed using particle image velocimetry (PIV).

†To whom correspondence should be addressed.
E-mail: maliang@ecust.edu.cn

EXPERIMENTS

1. Cyclone Separator

Aerosol sorting classifiers with heights of 4a, 5a, and 6a were selected as research objects; these sorting classifiers were connected with a cyclone. A sorting classifier at the inlet of the cyclone has a pre-classification function to the disordered particles due to the centrifugal effect, which will make the larger particles of the same density reach the outside entrance wall of the sorting classifier outlet more easily. A cyclone separator with no sorting classifier connected to its inlet is called a conventional cyclone (overlook clockwise, C-C). A cyclone separator equipped with a sorting classifier to make the larger particles closer to the outside entrance wall is called a positive rotation cyclone (PR-C). Conversely, it is called reverse rota-

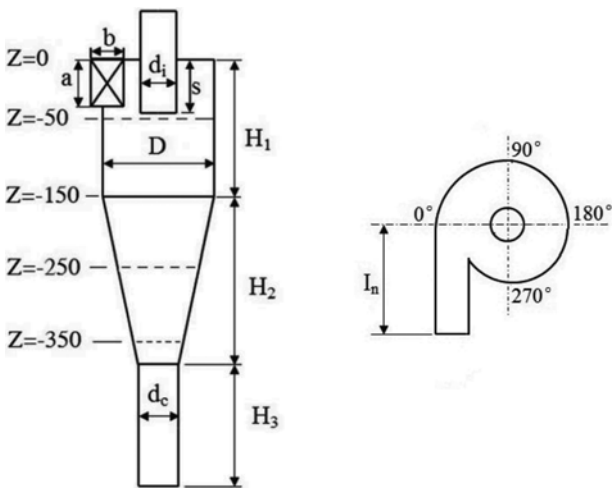

Fig. 1. Structural diagram of a conventional cyclone.

Table 1. Dimensions (mm) of a cyclone

D	d	a	b	d_i	d_c	S	h	H_1	H_2	H_3	I_n
75	30	45	30	35	38	50	220	150	225	150	100

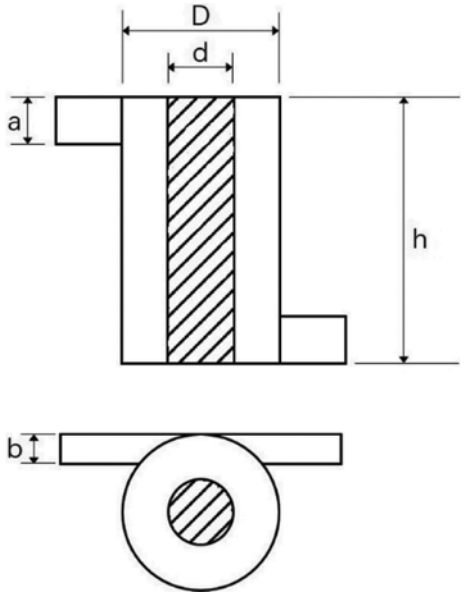

Fig. 2. Schematic plot of particle arrangement.

tion cyclone (RR-C). The cyclone separator used in this experiment is optimized on the basis of Stairmand high efficiency cyclone separator (diameter about 200 mm), cutting down the column diameter, which can strengthen the centrifugal effect, improving the separation efficiency of micron particles. The underflow diameter is greater than the inner diameter of vortex finder, which reduces the probability of back mixing at the bottom of the cone. Fig. 1 shows the structure of a C-C, and Table 1 shows the dimensions of the cyclone. In Fig. 1, Z=−50 refers to the section located 50 mm from the top of inlet. Fig. 2 shows the schematic of the sorting classifier, and Table 1 shows its dimensions. Fig. 3 shows the three types of separator series.

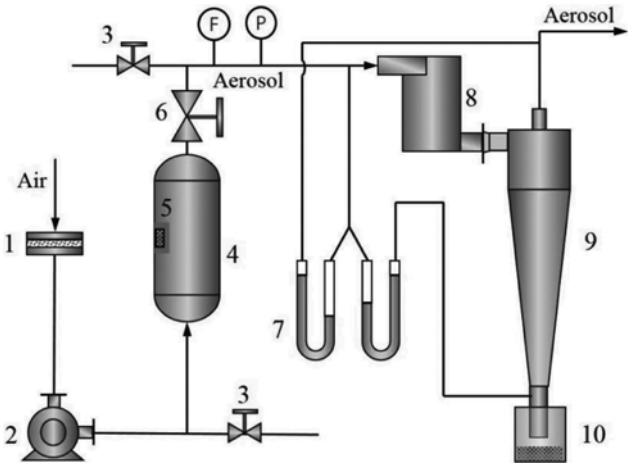

Fig. 4. Flow chart of the experiment.

1. Air filter
2. Roots blower
3. Bypass valve
4. Blending tank
5. Feeder
6. Throttle valve
7. U-tube manometer
8. Sorting classifier
9. Cyclone separator
10. Hopper

F. Flow meter
P. Pressure gauge

2. Experimental Procedure

At first the experimental system was checked to contain no impurities and its working status was smooth. Then weighted particles were added into the feeder before the blower was turned on and adjusted to the require working condition. After 15 minutes' steady operation, the feeding was started, and then the working condition parameters, including time, pressure and flow rate, were recorded. Afterwards, the aerosol particle concentration and separation efficiency were calculated by weight method. The experiments were repeated three times. In addition, data sampling was conducted in all the three repeated experiments and the results were averaged before display. Fig. 4 shows that under normal pressure and temperature, air was filtered by an air filter (1) and then drawn in by a roots blower (2). The roots blower increased the force

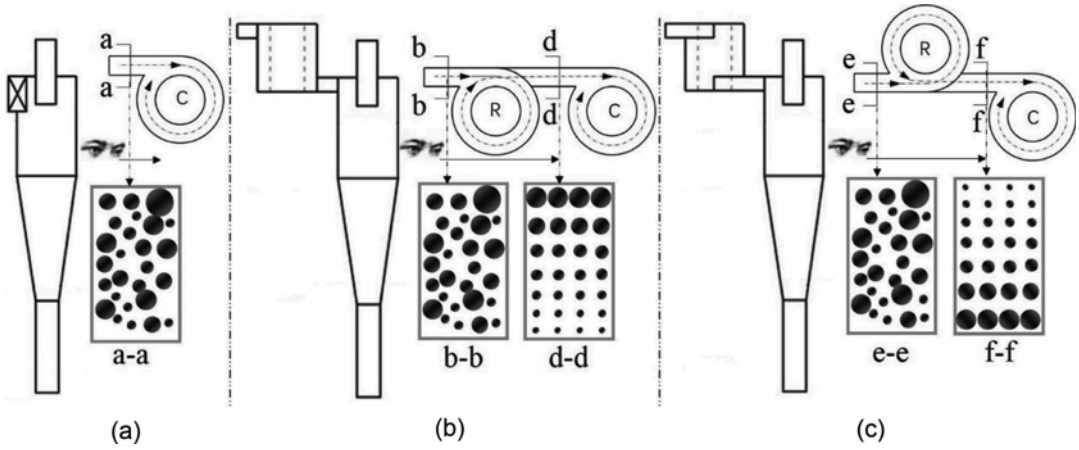

Fig. 3. Three kinds of separator series and diagram of inlet particle distribution (R - regulator; C - cyclone).
(a) Conventional cyclone, (b) positive rotation cyclone, (c) reverse rotation cyclone

Table 2. Major equipment used in this experiment

Name	Quantity	Type and specification	Manufacturer (accuracy and range)
Air filter	1	AST-01	Shanghai Songtai Purification Technology Co., LTD.
Roots blower	1	GHBH 001 34 1R4	Gauri High-pressure Blower Company in Germany
Bypass valve	2	Q25F-16P	Shanghai Jvguang Valve Co., LTD.
Blending tank	1	0.15 m^3	Design by ourselves
Shaking feeder	1	10 g/h	Design by ourselves
Throttle valve	1	Q50F-16P	Shanghai Jvguang Valve Co., LTD.
U-tube manometer	2	100×600, φ10	Design by ourselves
Separator	1	D=75	Design by ourselves
Sorting classifier	6	4a, 5a, 6a	Design by ourselves
Hopper	1	φ80×200	Design by ourselves
Flow meter	1	KKF83E	Shanghai Wuhuan Instrument Co., LTD. Accuracy: ±0.5%, Range: 10-300 m^3/h.
Pressure gauge	1	DPG A-04	Dwyer Instruments, Inc. Accuracy: ±0.7%, Range: 0-0.3 Mpa.
Electronic balance	1	BSM 2204	Shanghai Zhuo Jing Electronic Technology Co., Ltd. Accuracy: 0.1 mg, Range: 0-120 g.

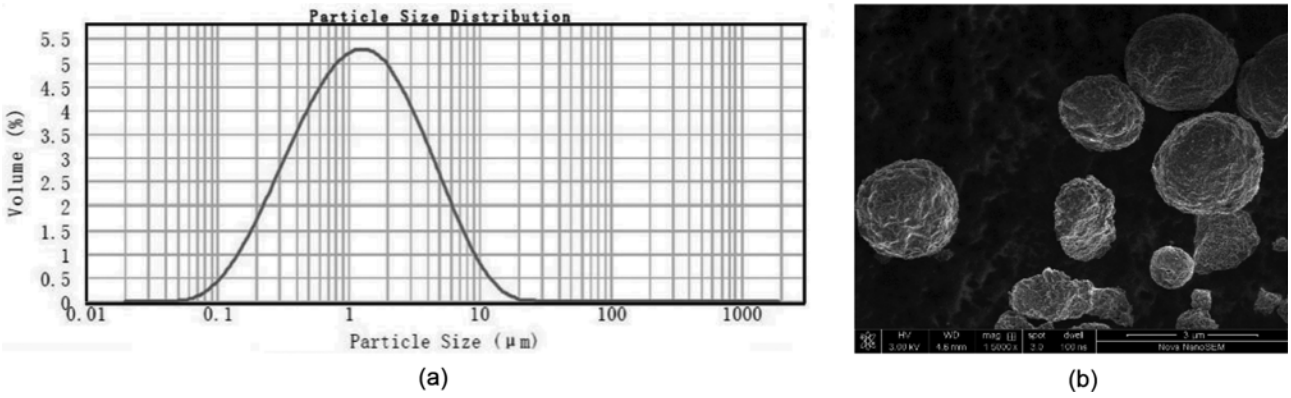

Fig. 5. (a) Particle size-volume distribution, (b) powder SEM image.

and velocity, resulting in complete mixing of air and solid particles, which came from shaking feeder (5) in the blending tank (4); consequently, the flow was stabilized. The required gas flow, flow velocity, and pressure were achieved by adjusting the throttle valve (6) and the bypass valve (3). The required parameters were measured using a pressure gauge P, a flow meter F, and a U-tube manometer (7). Particles proceeded into a cyclone separator (9) after being arranged by a sorting classifier (8) and then separated into a hopper in the underflow. The gas was subsequently drained directly after cleaning.

3. Experimental Material

The experimental material was an aerosol mixture of air and catalyst particles, which were provided by Shanghai Xiangtian Nano Material Co., Ltd. By adjusting the shaking feeder, the weight per unit time of the materials added in the air was changed to maintain the concentration of solid particles at 2 mg/L and the temperature at 20 °C under different flow velocity. The air served as continuous phase with a density of 1.205 kg/m^3 and a viscosity of 0.000018 Pa·s. The catalyst particle is the dispersion phase with a density of 893 kg/m^3 and a particle size of 0.05-30 μm. Figs. 5(a) and 5(b) show the size distribution and SEM image of the catalyst particle, respectively. The major equipments used in this experiment are showed in the Table 2.

4. PIV Test of the Separator Flow Field

PIV is a new type of measurement method for the precise determination of flow field that has rapidly developed in recent years. It avoids disturbing the fluid flow field and has a full-view measurement in an instant time. Variation in tangential velocity in the inner flow field of the C-C, PR-C, and RR-C was measured with the height of 5a and the velocity of 30, 40, or 50 m^3/h. The tangential velocity value is obviously greater than that of the axial velocity and the radial velocity. The centrifugal force field, which is produced by the tangential velocity, is the precondition of the separation of aerosol particle by the swirling flow field. The centrifugal force field exerts an important effect on separation efficiency. When Z=−50, the cross section is closer to the inlet and the overflow. The distribution of the tangential velocity is more complex or disordered, reflecting the obvious effect of sorting classifier on inner flow field of the cyclone

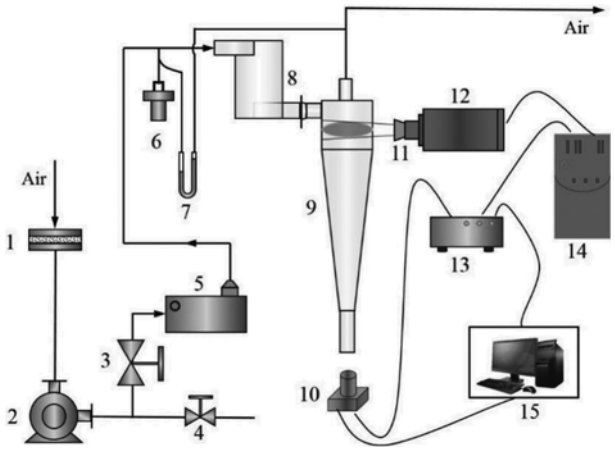

Fig. 6. PIV experimental flow chart.

1. Air filter
2. Regenerative blower
3. Throttle valve
4. Bypass valve
5. Atomizer
6. Pitot tube
7. U-tube manometer
8. Sorting classifier
9. Cyclone
10. CCD camera
11. Light sheet optics
12. Dual YAG laser
13. Synchronizer
14. Laser controller
15. Computer system

separator.

Fig. 6 shows the PIV testing process. The regenerative blower served as power source. Filtered air served as continuous phase, and the required gas flow was obtained by using a throttle valve and a bypass valve. The tracer particles were obtained using a atomizer (BX-03B) to atomize 5 wt% sugar solution under normal temperature and pressure and produce an average particle size of 0.8 μm (sugar particle density of 1.58×103 kg/m^3, refractive index 1.54), whose concentration can be reduced or increased by controlling the number of atomizer. The tracer particles were carried into the cyclone separator by the air after being sorted by the sorting classifier. A pitot tube and a U-tube manometer were set before and after the separator to measure the total pressure and the front-back pressure drop. The relevant intensity schistose laser source was emitted from the laser controller and transferred to a 2 mm light sheet by using compound light sheet optics. The laser sheet directly irradiated the cross-sections of the cyclone. A CCD camera collected image at the bottom of the cyclone, and the images were sent into a computer. The computer controlled the laser and collected images with the help of a synchronizer. The PIV system tested the tangential velocity at the cross-sectional flow field (Z=−50) with the flow values of 30, 40, or 50 m^3/h.

RESULTS AND DISCUSSION

The performance indices of the cyclone separator mainly include operation index and separation index. The operation index refers to the pressure, flow, pressure drop, temperature and concentration. Separation index refers to classification efficiency, separation efficiency, among others. In the flow field of a cyclone separator, the centrifugal force field, which is generated by tangential velocity, is the precondition for the separation of aerosol particles and greatly influences the separation property of the cyclone operator.

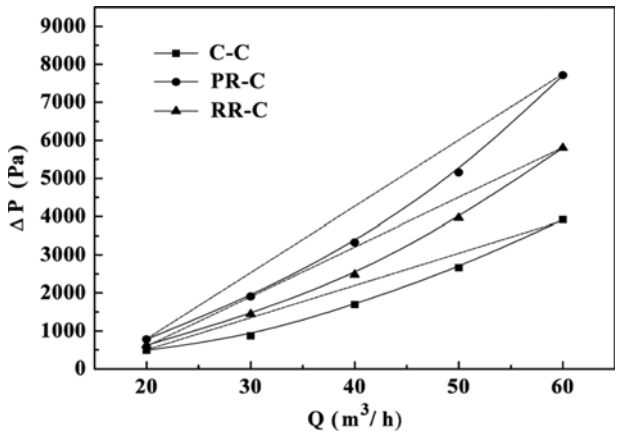

Fig. 7. Flow-pressure drop relationship (h=4a).

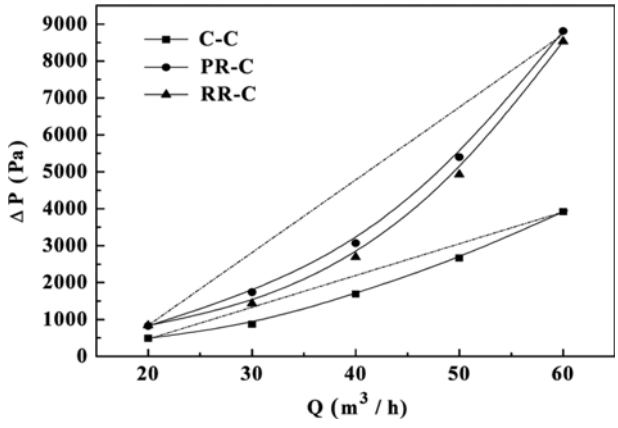

Fig. 8. Flow-pressure drop relationship (h=5a).

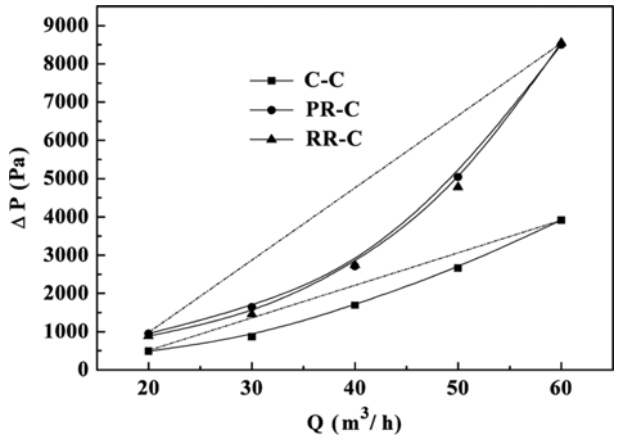

Fig. 9. Flow-pressure drop relationship (h=6a).

1. Effect of Sorting Classifier on Pressure Drop

A low pressure drop reduces energy consumption, and transformation of systemic draught fan is unnecessary while adding the sorting classifier before the cyclone separation equipment. Figs. 7, 8, and 9, respectively, refer to the aerosol sorting classifiers with heights of 4a, 5a, and 6a. Under different flow conditions, the

flow-pressure drop relationships are as follows.

The figures show that the pressure drops in C-C, PR-C, and RR-C increased with increasing inlet flow. Under the same flow, pressure drop in the three cyclone separators decreases in the following order: PR-C>RR-C>C-C. Thus, addition of aerosol sorting classifier increases the total energy consumption. When flow is small, the pressure drops in the three cyclone types are nearly the same. However, as the flow increases, the progressive increase ranges of the PR-C and the RR-C are obviously greater than that of the C-C. With the increased height of the sorting classifier, the difference in pressure drop between the PR-C and the RR-C gradually decreases. Under high flow, pressure drops are nearly the same. When the velocity of air suction is lower than 40 m^3/h, pressure drops in PR-C and the RR-C are 1,000 Pa lower than that in the C-C. Although the addition of the sorting classifier will increase the pressure drop, it is less than 3,000 Pa, which is still a low pressure drop for industrial applications.

2. Effect of Sorting Classifier on Separation Efficiency

M_i, M_u, and M_o represent the quality of the inlet particle, the trapping particle, and the escaping particle, respectively. Separation efficiency E is expressed as follows:

$$E=\frac{M_u}{M_i}=1-\frac{M_o}{M_i}=\frac{M_u}{M_u+M_o}$$

Under similar work condition, the separating property of the three kinds of separators was determined by changing only the trance flow. Figs. 10, 11, and 12 show the separation efficiency of the three separators with different inlet flows, and the heights of the sorting classifiers are 4a, 5a, and 6a.

Figs. 10, 11, and 12 show that whether the height of the sorting classifier increases or not, the separation efficiency of the three separators increases with increased inlet flow first; this phenomenon is caused by low centrifugal force in the interior of the cyclone separator under a small flow condition. The migratory power of the particle of the dispersion phase to the sidewall and the separation efficiency are low. When inlet flow is added, the centrifugal force and the efficiency of the cyclone separator increase gradually at first. When the particles reach the wall of the cyclone that represents solid particles are separated, and the RR-C separator sorts the particles which can make the smaller particles closer to the outside wall at the entrance of the cyclone separator, it strengthens the separation efficiency of small particles. When the maximum efficiency is reached, the efficiency will subsequently decrease, because the particle stays in the cyclone separator for a shorter time as the inlet flow continuously increases and causes the increment in the short-circuit current. Moreover, the increment in the intensity of inner flow turbulence disrupts the relatively organized field between forced vortex and free vortex in the inner flow field, reducing the separation efficiency, but the rate of decrease of RR-C is the slowest. The highest separation efficiency of the RR-C is higher than that of the C-C by approximately 3%-5%, whereas the highest separation efficiency of the C-C is higher than that of the PR-C by approximately 1.5%. This result was obtained because the PR-C increases the particles in larger granularity close to the outside wall at the inlet of the cyclone, whereas the RR-C increases the particles in larger granularity close to inside wall at the inlet of the cyclone. Thus, with the use of the same material under similar separation accuracy, particle granularity and concentration on the inlet cross section changes

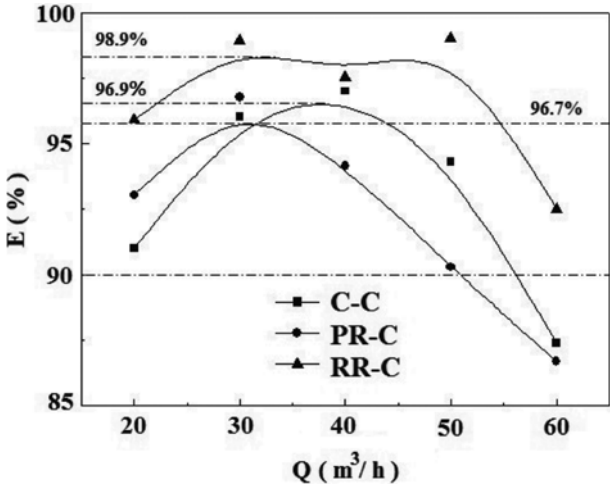

Fig. 10. Collection efficiency (h=4a).

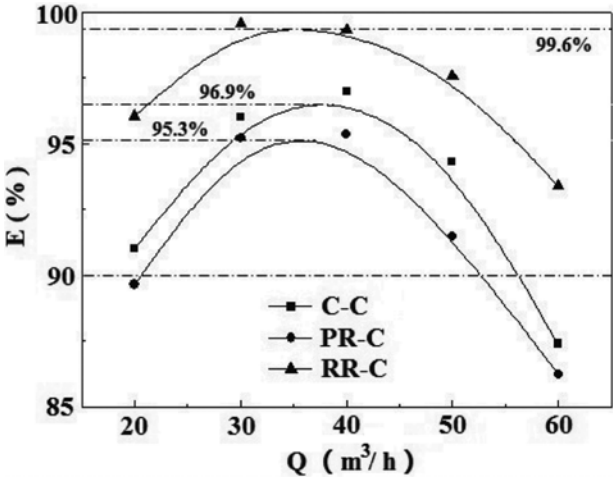

Fig. 11. Collection efficiency (h=5a).

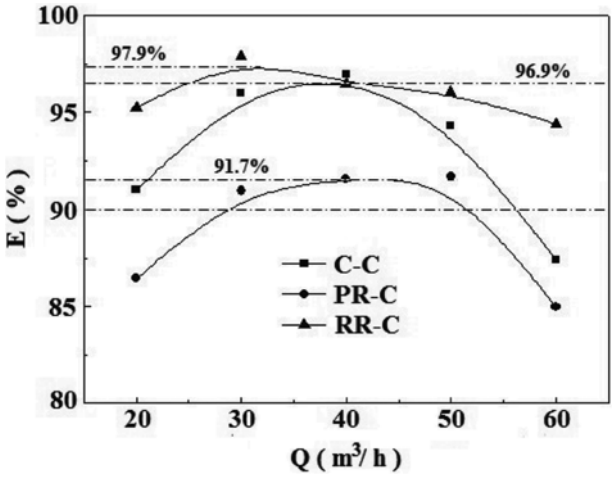

Fig. 12. Collection efficiency (h=6a).

after aerosol particle sorting, and the effect of particle distribution on efficiency is larger than that on concentration. Size greatly affects the efficiency of separation of small particles; the closer the smaller particles are to the outside wall at the inlet of the cyclone, the higher the separation efficiency will be.

The flow related to the maximum efficiency of the RR-C is smaller than that of the C-C and PR-C. This finding indicates that with the same other parameters, it is easy for the RR-C with the sorted aerosol particle to get the top efficiency separation. In the efficient separation field, wherein the separation efficiency is higher than 90%, the separation efficiency of the RR-C must be greater than that of the two other cyclone separators. Thus, the efficient separation field increases when aerosol particles are sorted. The increase of the efficient separation field of the separators is conducive. Moreover, the operating flexibility will increase.

For the PR-C, the separation efficiency decreases as the height of the sorting classifier increases, and all the separation efficiency is lower than the C-C. For the RR-C, the separation efficiency increases first and then decrease with the increase of the height of the sorting classifier; when the height is 5a, the separation efficiency reaches the highest, and all the separation efficiency is higher than the C-C.

3. Effect of Sorting Classifier on Grade Efficiency

Separation efficiency is related to not only the working condition, dimension parameter, and material density during operation, but also to the diameter of the separated aerosol particle. Thus, a grade efficiency curve is often used to forecast the separation property of a cyclone separator.

To the particle group at the inlet, underflow and overflow, if the corresponding mass distribution functions are fi (x), fu (x) and fo (x), when the sorter height is 5a, the inlet velocity is 40 m^3/h, the particles concentration is 2.0 mg/L, sampling and weighing the particles from the inlet, underflow, overflow of the C-C, RR-C and PR-C respectively in 10 minutes, the inlet mass (m_i), underflow mass (m_u), overflow mass (m_o) of each cyclone can be gained, and the volume size distribution and proportion (w_i, w_u, w_o) of specific size particles from inlet, dust outlet and gas outlet of three cyclones can also be obtained by using Malvin particle size analyzer. Because the same mass density of particles, according to the specific volume distribution and proportion, the corresponding mass value of the $fi(x)=m_i \times w_i(x)$, $fu(x)=m_u \times w_u(x)$ or $fo(x)=m_o \times w_o(x)$ can also be obtained.

Then the particle size is between x−0.5dx and x+0.5dx, and the mass balance is: fi (x)dx=E fu (x)dx+(1−E) fo (x)dx=dFi(x)=E dFu (x)+(1−E) dFo (x). Therefore, the mass balance equation can be obtained for the aerosol particles smaller than the given particle size x: Fi(x)=E Fu (x)+(1−E) Fo (x), The classification efficiency can be defined as the aerosol particle size between x−0.5dx and x+0.5dx, and the ratio of the particles separated from the rotating centrifuge separator to the particles entering the separator: G(d)= Mu fu (x)dx/Mi fi (x) dx.=1-(1−E)[dFo (x)/d fi (x)].

Fig. 13 show the grade efficiency curve when the height is 5a and the inlet flow is 40 m^3/h. The figure shows that for a small particle (generally smaller than 0.8 μm), the grade efficiency of the RR-C is higher than that of the C-C, whereas the PR-C shows the lowest grade efficiency. This result indicates that granularity of particles in the inlet is distributed in descending order from the inside wall to the outside wall by the RR-C, and this phenomenon is beneficial for the smaller particles to be separated and gathered in the hopper at underflow. The grade efficiency curve of the PR-C is steeper than that of the other cyclones; thus, the PR-C demonstrates a more obvious grade efficiency, and result is related to the particles' distribution in descending order from the outside wall to the inside wall at the inlet. The larger particles transport close to the outside wall and tend to separate into the hopper at underflow, whereas smaller particles close to the inside and tend to enter into the overflow and thus are hard to separate.

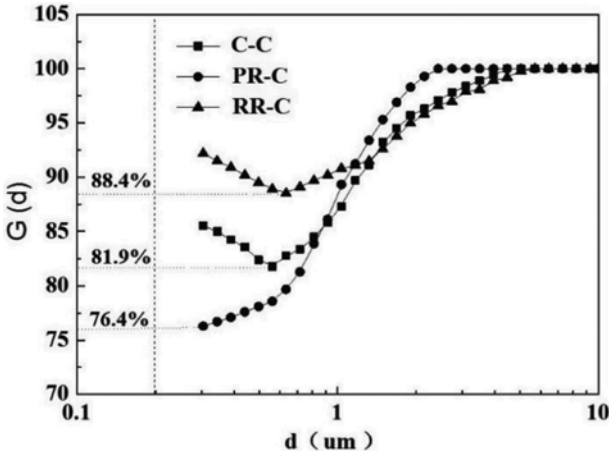

Fig. 13. Grade efficiency of the three types of cyclone under h=5a and Q=40 m^3/h.

The grade efficiency curve of the C-C obviously demonstrates a fishhook effect. When the aerosol particle is less than 0.6 μm, the grade efficiency increases. The grade efficiency curve of the RR-C also demonstrates a fishhook effect, which is not obvious at all. The main reason is that the tiny particles pass through the aerosol sorting classifier and are distributed on the outside wall from the column section of the cyclone. The tiny particles reduce the upper fishhook effect by reuniting at the inlet. In the PR-C, a large amount of tiny particles is located close to the axis. It gets to the overflow pipe with the short-circuit current flow field and away from the separator before the aggregation effect (or with the weak aggregation effect), which disrupts the fishhook effect. Under a large particle grade efficiency (approximately larger than 1 μm), the PR-C effectively increases the grade efficiency of this part. For particles larger than 5 μm, the grade efficiency of the three kinds of cyclone nearly reaches 100%. But in the experiment, some particles (larger than 5 μm) escape inevitably, and so the approximate treatment involving 100% grade efficiency is used in this study.

4. Separation Efficiency to Coefficient-of-pressure

A non-dimensional parameter like the ratio of E/ΔP can be used for comparing the different designs. The pressure drop and separation efficiency are two important indexes to evaluate the performance of cyclone separator. When the separation efficiency of the cyclone separator is higher or the pressure drop is lower, the performance of the cyclone separator is better.

In the Fig. 14, the E/ΔP is the highest when there is no sorting classifier, which is 2 to 3 times when there is a sorting classifier. This is because the addition of the sorting classifier increases the

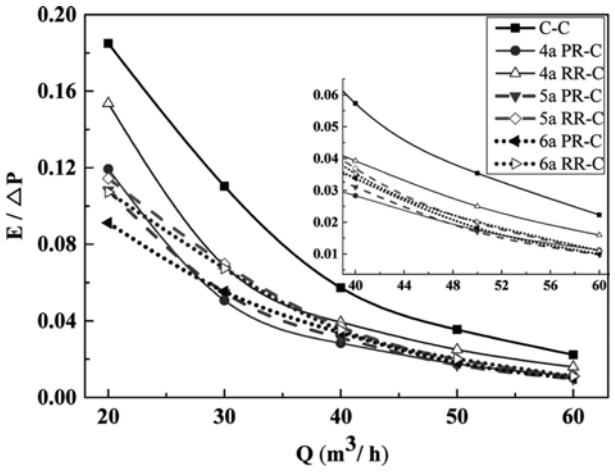

Fig. 14. Relationship between the Q and E/ΔP.

pressure drop and separation efficiency, but the increase in pressure drop is significantly higher than the separation efficiency. We can see from the graph that the E/ΔP decreases as the height of the sorting classifier increases, because the higher the height of the sorting classifier is, the higher the pressure drop is under the same flow. When at the same height of the sorting classifier, the E/ΔP of RR-C are all higher than PR-C, which shows that the comprehensive performance of RR-C is better than PR-C.

5. Analysis of Tangential Velocity

Figs. 15(a), 15(b), and 15(c) show the tangential velocity distribution of the three kinds of cyclones under different flow conditions when Z=−50. The tracer particles in PIV test represent the continuous phase. The figures show that the inlet flow rate exerts little effect on the regularity of distribution of the tangential velocity but on the velocity value. Regularities in distribution of the tangential velocity are nearly the same, wherein they generally present axial symmetry.

The tangential velocity speeds up from the sidewall to the axis along the radial direction, and nearly all tangential velocities in the axis are close to zero. As flow increases, the tangential velocity is more amplified in the PR-C and RR-C than in the C-C. Moreover, the tangential velocity of the RR-C is more amplified than that of the PR-C. All of the results above show that under the same flow, the RR-C demonstrates a stronger centrifugal separating power, and the distribution of its tangential velocity is more stable than that in the two other cyclones. The test result obtained in the flow field is consistent with the experimental result.

Figs. 16(a), 16(b), and 16(c) show that when at the same flow rate, RR-C is more stable and less volatile. PR-C is characterized by high volatility and irregular velocity. It is easy to produce particle mixing in the flow field, so the separation efficiency is reduced. At the same section, with the increase of intake speed, the tangential velocity of RR-C increases fastest, so the separation efficiency is improved.

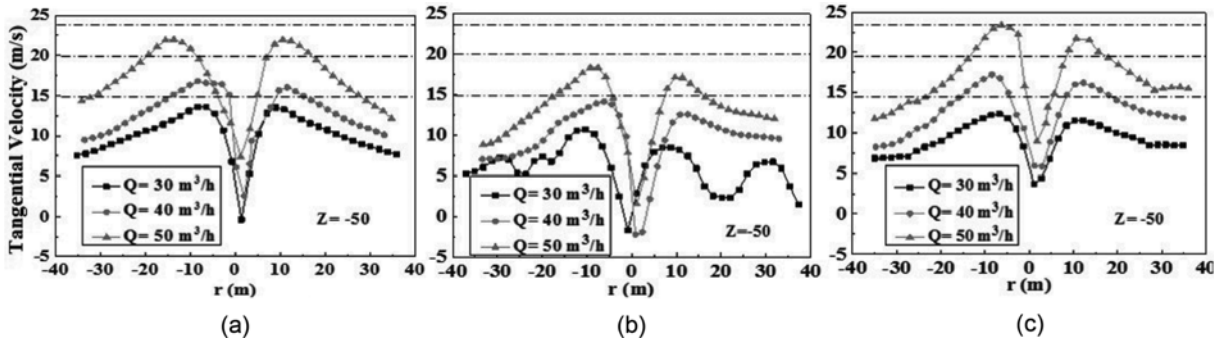

Fig. 15. Tangential velocity distribution of C-C, PR-C and RR-C at different inlet velocity.
(a) Tangential velocity of C-C, (b) tangential velocity of PR-C (c) tangential velocity of RR-C

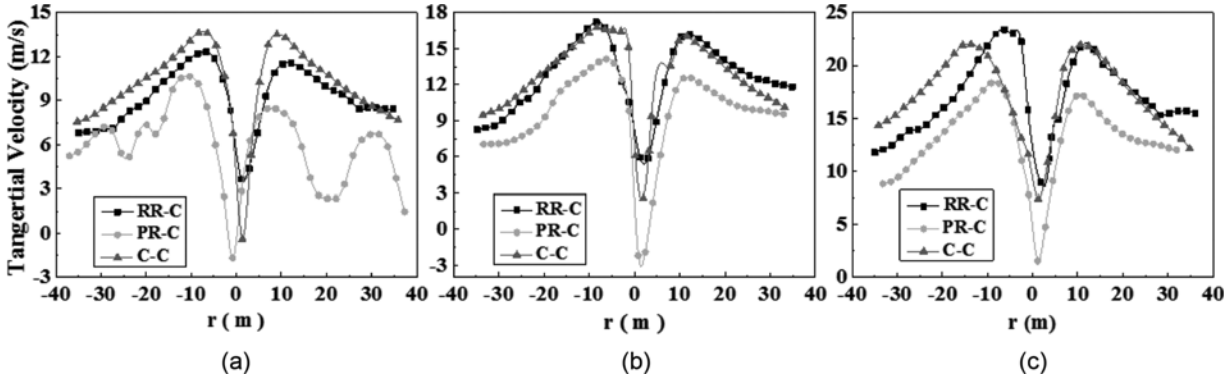

Fig. 16. Tangential velocity distribution of C-C, PR-C and RR-C at same inlet velocity.
(a) Inlet velocity is 30 m³/h, (b) inlet velocity is 40 m³/h, (c) inlet velocity is 50 m³/h

CONCLUSION

Pressure drop in the three types of cyclones increases with increased inlet flow. The progressive increase in the PR-C and in the RR-C is obviously greater than that in the C-C. The pressure drop and the energy consumption are increased by adding aerosol particle sorting classifier. The pressure drop and the energy consumption are nearly the same under a large flow working condition. When the flow rate of the air suction is lower than 40 m^3/h, the amplification of the pressure drop of the PR-C and the RR-C is lower than 1,000 Pa compared with that of the C-C.

Sorting of inlet aerosol particle directly influences the separation efficiency of the cyclone separator. The separation efficiency is highest in RR-C, successively followed by that of the C-C and PR-C. Smaller particles close to the sidewall are separated easily, but the smaller particle close to the axis enters into the overflow easily. The inner flow field, which is affected by the RR-C particle sorting classifier, is more stable, and amplification of the tangential velocity is larger, which is beneficial for particle separation. The testing result obtained in the flow field corresponds to the experimental result.

The grade efficiency of the conventional cyclone demonstrates an obvious fishhook effect; the fishhook effect of the RR-C separator is weak, whereas no fishhook effect was observed in the PR-C. The RR-C separator and PR-C demonstrate an enhanced separating property for the tiny particles smaller and greater than 1 μm, respectively. The RR-C has a superior overall separating property, but the PR-C demonstrates a higher classification effect than the RR-C.

ACKNOWLEDGEMENTS

We would like to express our thanks for the sponsorship of National Key Research and Development Program of China (2016YFC0204500), National Natural Science Foundation of China (51608203), Shanghai Rising-Star Program (17QB1400300), and Science and Technology Commission of Shanghai Municipality (16dz1206400).

REFERENCES

1. J. C. Chow, J. G. Watson, J. L. Mauderly, D. L. Costa and R. Wyzga, *J. Air Waste Manage. Assoc.*, **56**, 1368 (2006).
2. Z. Antonella and S. Joel, *Environ. Health Persp.*, **117**, 898 (2009).
3. B. Michael, F. Greg, J. F. Joseph and C. Aaron, *Environ. Sci. Technol.*, **50**, 79 (2016).
4. S. Movafaghiana, J. A. Jaua-Martureta, R. S. Mohana, O. Shohama and G. E. Koubab, *Int. J. Multiphas Flow*, **26**, 999 (2000).
5. Y. H. Zhang, A. L. Liu, L. Ma and Y. M. Wang, *Aerosol. Air Qual. Res.*, **16**, 2287 (2016).
6. L. Ma, J. P. Wu, Y. H. Zhang, Q. S. Shen, J. P. Li and H. L. Wang, *Aerosol. Air Qual. Res.*, **14**, 1675 (2014).
7. L. Ma, Q. S. Shen, J. P. Li, Y. H. Zhang, J. P. Wu and H. L. Wang, *Chem. Eng. Technol.*, **37**, 1072 (2014).
8. L. Ma, Q. Yang, Y. Huang, P. Qian and J. G. Wang, *Chem. Eng. Technol.*, **36**, 696 (2013).
9. C. W. Haig, A. Hursthouse, S. McIlwain and D. Sykes, *Powder Technol.*, **258**, 110 (2014).
10. C. C. Gutierrez-Torres, P. Quinto-Diez, J. A. Jimenez-Bernal, A. Lopez-Lobato and J. G. Barbosa-Saldaña, *Int. J. Miner. Process*, **102**, 156 (2012).
11. K. Elsayed and C. Lacor, *Appl. Math. Model.*, **35**, 1952 (2011).
12. D. Misiulia, A. G. Andersson and T. S. Lundström, *Chem. Eng. Res. Des.*, **102**, 307 (2015).
13. F. P. Qian and Y. P. Wu, *Chem. Eng. Res. Des.*, **87**, 1567 (2009).
14. A. Wang, X. K. Yan and L. J. Wang, *Sep. Purif. Technol.*, **149**, 308 (2015).
15. C. Y. Hsu and R. M. Wu, *Dry Technol.*, **28**, 916 (2010).
16. P. B. Fu, F. Wang, L. Ma, X. J. Yang and H. L. Wang, *Sep. Purif. Technol.*, **158**, 357 (2016).
17. P. B. Fu, F. Wang, X. J. Yang, L. Ma, X. Cui and H. L. Wang, *Environ. Sci. Technol.*, **51**, 1587 (2017).
18. L. Ma, P. B. Fu, J. P. Wu, F. Wang, J. P. Li, Q. S. Shen and H. L. Wang, *Aerosol. Air Qual. Res.*, **15**, 2456 (2015).
19. Q. Yang, W. J. Lv, L. Ma and H. L. Wang, *Sep. Purif. Technol.*, **102**, 15 (2013).
20. Y. Hiraiwa, T. Oshitari, K. Fukui, T. Yamamoto and H. Yoshida, *Sep. Purif. Technol.*, **118**, 670 (2013).
21. Z. B. Wang, L. Y. Chu, W. M. Chen and S. G. Wang, *Chem. Eng. J.*, **138**, 1 (2008).
22. P. K. Liu, L. Y. Chu, J. Wang and Y. F. Yu, *Chem. Eng. Technol.*, **31**, 474 (2008).
23. Y. Xu, J. G. Wang, S. L. Zhao and Z. S. Bai, *Chem. Eng. Res. Des.*, **94**, 691 (2015).
24. J. G. Wang, Z. S. Bai, Q. Yang, Y. Fan and H. L. Wang, *Sep. Purif. Technol.*, **163**, 120 (2016).